

Finite Element Analysis (FEA) of blade weed design using Ansys workbench

Angger Bagus Prasetyo^{1*}, Rizqi Prastowo², Kartinasari Ayuhikmatin Sekarjati³, Anita Susiana⁴, Ichwan Noor Ardiyat⁵, Fajar Yulianto Prabowo⁶, Iman Pradana A. Assagaf⁷, Jemssy Ronald Rohi⁸, Yonathan Ito⁹

¹Department of Mechanical Engineering, Faculty of Industrial Technology, Institut Teknologi Nasional Yogyakarta, Indonesia

²Department of Mining Engineering, Faculty of Mineral Engineering, Institut Teknologi Nasional Yogyakarta, Indonesia

³Department of Industrial Engineering, Faculty of Industrial Technology, Institut Sains & Teknologi AKPRIND, Indonesia

⁴Department of Mechanical Engineering, Faculty of Technology, Universitas Prof. Dr. Hazairin, SH., Indonesia

⁵Department of Mechanical Engineering, Politeknik Negeri Banjarmasin, Indonesia

⁶Department of Mechanical Engineering, Faculty of Industrial Technology, Institut Sains & Teknologi AKPRIND, Indonesia

⁷Department of Agro Industry Manufacturing Engineering, Politeknik ATI Makasar, Indonesia

⁸Department of Mechanical Engineering, Faculty of Technology, Universitas Pertahanan RI, Indonesia

⁹Department of Mechanical Engineering, Faculty of Technology, Universitas Perwira Purbalingga, Indonesia

Abstract

Manual, semi-conventional, and conventional weed eradication are the three forms of weed eradication utilized. Farmers benefit greatly from the usage of weeding equipment in combating pests in the fields. The blade you use determines how successful you are at weeding. As a result, it is required to examine the weeding weeds blade. With a tetrahedral mesh, simulation utilizing the finite element analysis approach allows for the optimization of design, computation, and prediction of material strength. The goal of this research was to figure out how much von Mises's stress, deformation, and safety factor were worth. ANSYS Workbench software was used to simulate various loadings of 10N, 25N, and 50N. The highest von Mises stress created by simulation of modelling weed blades at 10N, 25N, and 50N loads is around 2.95×10^{-2} MPa, 7.38×10^{-2} MPa, and 0.14755 MPa, respectively. Each of the safety factors is 15, and the maximum deformation value is 4.26×10^{-7} mm; 1.06×10^{-6} mm; 2.13×10^{-6} mm. The safety factor indicates that the weed weeding knife design is safe to use up to 50N loading.

This is an open-access article under the [CC BY-NC](#) license



Keywords:

Ansysis;
Finite Element Analysis;
Tetrahedral mesh;

Article History:

Received: February 23, 2022

Revised: May 19, 2022

Accepted: May 23, 2022

Published: October 14, 2022

Corresponding Author:

Angger Bagus Prasetyo
Mechanical Engineering
Department, Institut Teknologi
Nasional Yogyakarta
Email:
anggerbprasetyo@gmail.com

INTRODUCTION

Mechanical equipment with a series of blades mounted on a revolving s is frequently used to cultivate soil [1]. One of the best methods to develop land is through intensification. Farmers must also look for an acceptable method/breakthrough to boost rice productivity, such as altering the space between rice and removing weeds. Weeds are one of the plant species that prevent rice plants from growing [2].

There are three types of weed eradication methods now on the market: manual (hand),

semi-automated, and conventional. In one rice-growing season, weeding is done twice. Weeding by hand consumes a lot of energy and takes a long time [3]. Semi-weeding is done with tools and a manual drive, whereas traditional weeding is done with tools and machine power. This provided the impetus for the development of a prototype weed weeder to support farmers in the effective and efficient eradication of weed pests. The weed weeding machine is made up of numerous parts, one of which is a weeding knife. The weeding machine's blade has a significant impact on the weeding performance.

The initial step in the machine-building process is to create a design. Machine design that incorporates recent technical advancements can drastically cut expenses [4].

Design optimization is required to reduce production defects and increase blade life, resulting in reduced idle time [5]. The blade is the determining factor in the success of the weed weeding operation [6]. As a result, it is required to examine the weeding weeds blade. The method of Finite Element Analysis (FEA) is used to analyze stresses and other characteristics [7]. Optimizing the design, performing theoretical calculations, forecasting the strength of a material [5], [8] and confirming the loading force with regression analysis [9] are all advantages of Finite Element Analysis (FEA). The design is capable of cutting, and the structural analysis is good, according to prior research examining the optimization of the blade by numerical simulation [10]. Numerical simulation has the advantage of being able to make quick forecasts without the need for field testing [11], [12].

The goal of this study is to design a modelling weed blade utilizing the Finite Element Analysis (FEA) approach and the ANSYS workbench to analyze the stress and strength of the weeding blade, based on the following explanation of the challenges. The determination of stress levels is critical in the design of agricultural machinery [13]. The interaction between the soil and the agricultural equipment determines the degree of tension on the tilling machine [14]. The nature of the soil, the form and size of the claws, and extra accessories all influence the stress level [15]. The study's findings include von Mises stress, displacement, and the safety factor.

METHOD

Design

CAD software was used to model the weed weeding blade. It is then saved in *.iges format so that the ANSYS Workbench software can read it. The blade design is generally determined by the weeding machine's mechanism holder. Table 1 shows the shapes and dimensions of the blade design. Figure 1 depicts the weed weeding machine model. Figure 2 depicts the design of the weed weeding blade. The shape utilized alters the degree of usability. Manufacturing and customizing marijuana weed knives.

Table 1. Size of weed blade geometry	
Geometry	Value
Long	37,35 mm
Wide	8,19 mm
Thick	5 mm
Blade Length	71,81 mm

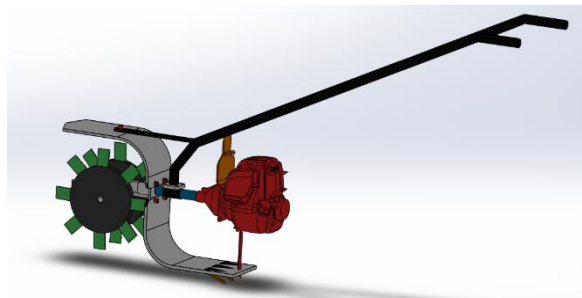


Figure 1. Design of weed weeding machine

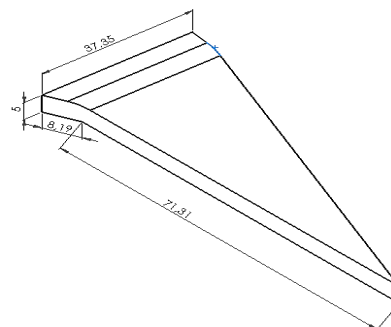


Figure 2. Weed weeding knife

Anslys Workbench

Anslys workbench is a simulation platform used by engineers to address engineering problems [16], including features such as material structural analysis, CFD analysis, heat transfer analysis, meshing, and engineering data [16]. The advantage of the Anslys workbench is that it can operate many solvers in one package with diverse interfaces, yet it is integrated into one system, such as CAD, CAM, and CAE, making it easier for engineers to construct geometric models [16], [17]. When conducting simulations, engineers must follow a number of procedures. According to [18], these steps include design, mesh division, boundary condition determination, and mathematical modeling.

Finite Element Analysis

Various phenomena in science and engineering may now be represented by employing a mechanical continuum to formulate differential equations. Due to the intricacy of material properties, boundary conditions, and the geometry of the structure itself, analytical solutions to partial differential equations are often difficult to acquire [19]. Numerical analysis utilizing the finite element method is one possible answer to such a challenge. By using numerical methods to generate approximate solutions, the finite element method converts partial differential equation problems into linear algebraic equations [20].

The finite element approach can be used to tackle a variety of issues, including physical ones. The finite element approach can be used to handle a variety of physical problems, including structural analysis problems, buckling, and vibration analysis [21]. The most common application of the finite element method is structural analysis. The term "structure" refers to structures other than buildings and bridges, such as aeronautical, naval, and mechanical ones. Structural analysis (static structural) ignores the effects of inertia and damping and considers displacements, stresses, strains, and forces on the structure as a result of loading. In the science of solid mechanics, analysis structure is extremely essential. The study of static structures can be linear or nonlinear [22]. A structure's failure can be investigated to reduce the error function, develop a stable solution, and solve engineering challenges [22].

Material

The structural steel material employed in this study for weed weeding blades has the qualities shown in Table 2. Structural steel was chosen since it is commonly utilized in the production of weed-whacking blades. For analysis, the data in the table will be entered into the ANSYS Workbench program. A 1.4 HP drive engine powers the weed weeding blades. Table 3 shows the parameters of the drive motor utilized in Mustang lawnmowers.

Meshing

Domain division or meshing has an impact on Finite Element Analysis (FEA) modelling [23]. Mesh is a simulation method with a high level of complexity [24]. The mesh results will have an impact on the simulation's convergence [25], [26]. Errors in meshing can be deadly, resulting in errors and simulation failures; if this happens, the mesh must be recreated.

Table 2. Blade mechanical properties

Properties	Value
Young's Modulus	2×10^5 Mpa
Poisson's Ratio	0,31
Density	7750 kg/mm^{-3}
Tensile Yield Strength	320 Mpa
Tensile Ultimate Strength	400 Mpa

Table 3. Condition of the blade at work

Parameter	value
Type Machine	150 cc
Spin Speed	6000 rpm
Power	1,4 Hp
Cilinder Contents	30,5 cc
Tank Capacity	1,2 litre

The results will be more accurate if the mesh is smaller, but the simulation procedure will take longer [27]. Hexahedral mesh, polyhedral mesh, and tetrahedral mesh are among the mesh types employed in CFD simulations [28], [29]. The tetrahedral mesh was employed in this study. As demonstrated in Figure 3, the usage of a tetrahedral mesh is preferable for stress distribution simulation [30] and is extensively utilized due to CFD modelling on irregular geometries [28].

Initial Condition

At this step, the constraints in the form of fixed support on the side and topsides must be determined; this was chosen because that section does not receive a fixed force, as seen in Figure 3. The knife is then thrust forward with vigour. The blade of the weeding machine will chop and weed the weeds that develop between the rice plants as it travels forward. The blade will be loaded during the weed cutting and weeding procedure, as shown in Figure 4. Figure 5 shows the force ones. The fluctuation of loads proposed in this study is based on this phenomenon (10 N, 25N and 50N). The simulation program is ready to run once the initial circumstances have been set. Von Mises stresses, deformations, and safety figures will be generated as a result of the simulation findings.

Mathematical Modeling

The simulation approach yielded parameters such as total deformation, equivalent stress, and safety factor. The following equation can theoretically be used to calculate the equation regulating the value of strain and stress:

$$\begin{Bmatrix} \sigma_{xx} \\ \sigma_{yy} \\ \sigma_{zz} \end{Bmatrix} = \frac{E}{(1+\nu)(1-2\nu)} \begin{Bmatrix} (1-\nu)\varepsilon_x + \nu\varepsilon_y + \nu\varepsilon_z \\ \nu\varepsilon_x + (1-\nu)\varepsilon_y + \nu\varepsilon_z \\ \nu\varepsilon_x + \nu\varepsilon_y + (1-\nu)\varepsilon_z \end{Bmatrix}$$

σ is stress, ε is strain, ν is poison ratio and E is young's modulus of a material.

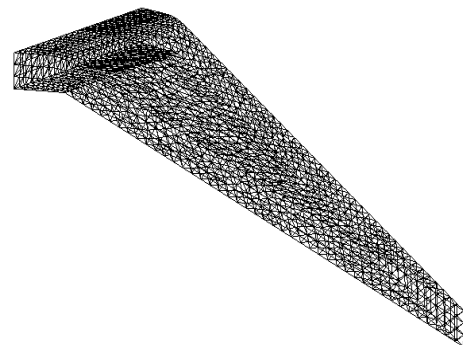


Figure 3. Tetrahedral mesh

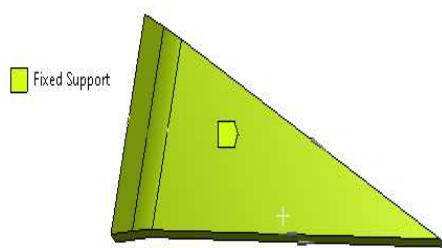


Figure 4. Fixed Support

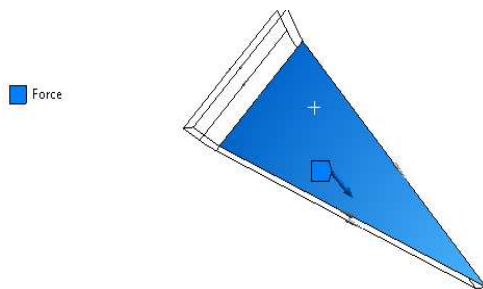


Figure 5. Force

While the following calculation can be used to get the safety factor value:

$$SF = \frac{\sigma_{max}}{\sigma_{max\ material}}$$

SF is a safety factor, σ_{max} is allowable material stress, $\sigma_{max\ material}$ is stress on the material.

RESULTS AND DISCUSSION

Von Mises Stress

There is pressure in an elastic object that functions in multiple directions [31]. Von Mises stress is a factor of whether a material is safe to use or whether it will fail throughout the process of use [32]. If the value of the von mises stress is greater than the material's strength, Von Mises can fail [33]. The von Mises stress distribution during operation is determined using the ANSYS Workbench software's analysis method for 10N, 25N, and 50N load changes. Figure 6, Figure 7, and Figure 8 illustrate the results of the simulation analysis of weeding blade modelling

In the simulation of modelling weeding blades with variations of 10N, 25N, and 50N, the maximum von mises stress values are around 2.95×10^{-2} MPa, 7.38×10^{-2} MPa, and 0.14755 MPa, respectively. While von Mises stress has a minimum value of 8.55×10^{-3} MPa, 2.14×10^{-2} MPa, and 4.28×10^{-2} MPa. Because the stress determination is directly proportional to the magnitude of the force received by an item, the maximum von mises value grows as the provided load increases [33].

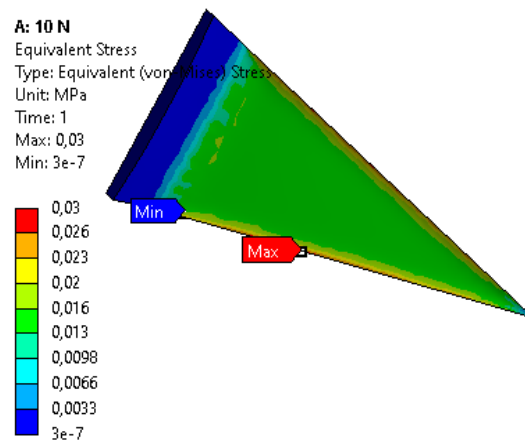


Figure 6. Von Mises Stress 10 N

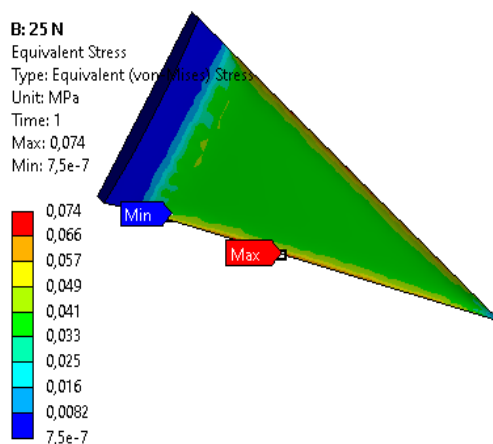


Figure 7. Von Mises Stress 25 N

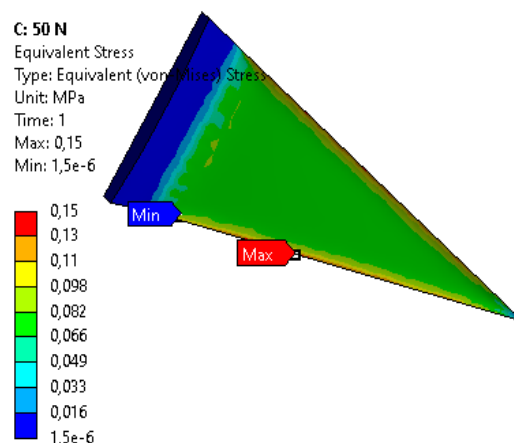


Figure 8. Von Mises Stress 50 N

Deformation

A key signal, namely deformation, can reveal the determinants of a material's strength and whether or not it can handle the load. The material's strength is proportional to its deformation value [34]. When an object is subjected to a force or a load, deformation can

occur [34]. Figure 9, Figure 10, and Figure 11 demonstrate the simulation results of modelling weeding blades.

In the simulation of weeding blades with loading changes of 10N, 25N, and 50N, the maximum deformation values are 4.26×10^{-7} mm, 1.06×10^{-6} mm, and 2.13×10^{-6} mm, respectively, while the minimum deformation value is 0. This demonstrates that the stronger the material is, the less the deformation [34]. The simulation findings show that even when the component is subjected to high stress, it does not deform significantly. The component will be damaged if it is unable to resist the applied load [35].

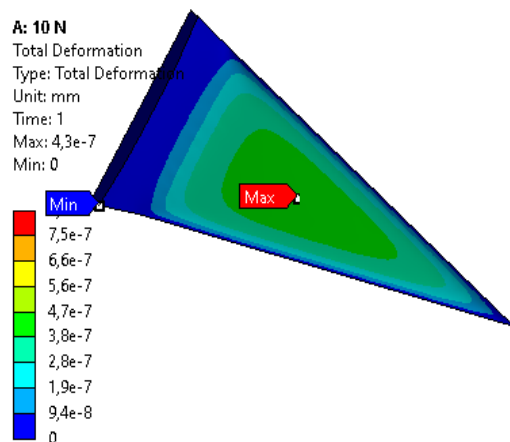


Figure 9. Deformation 10 N

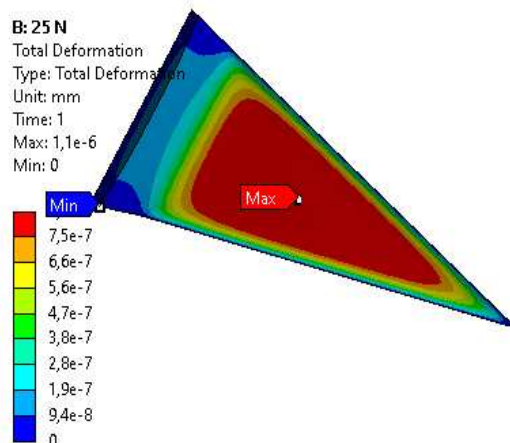


Figure 10. Deformation 25 N

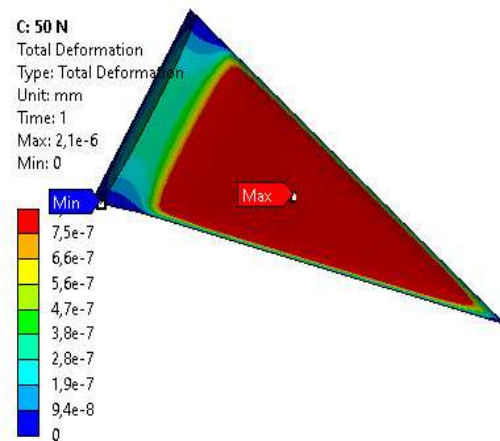


Figure 11. Deformation 50 N

Safety Factor

The lowest value of a design's safety factor [36] is a good measure of how safe it is to use. One of the factors used as a reference for stress testing on modelling an object is the safety factor [37]. Figure 12, Figure 13, and Figure 14 illustrate the outcomes of the modelling simulations. The blade modelling simulation findings demonstrate that the safety valve in the blade simulation is 15, indicating that the design described in this study is safe to use and fulfils the allowed safety values.

The safety factor of a good model is greater than one [33], [38]. The safety factor for a material capable of withstanding dynamic loads is usually between 2-3 [39]. The safety factor value is adequate to sustain shock loads [39]. Factor The safety factor is employed in the evaluation process to ensure that the proposed design is safe, and it becomes a measure of an element's strength [40]. In the design of a modelling simulation, numerous elements influence the safety factor [37]. The primary factors, according to researchers, are (a) the accuracy of the calculated load; (b) the usage environment; (c) the material's qualitative and craft factors; and (d) the need for plastic deformation and stiffness. [37]. In general, the safety factor value in this investigation met the standards for enduring dynamic loads. Loads that arise unexpectedly and change over time are known as dynamic loads [40][41].

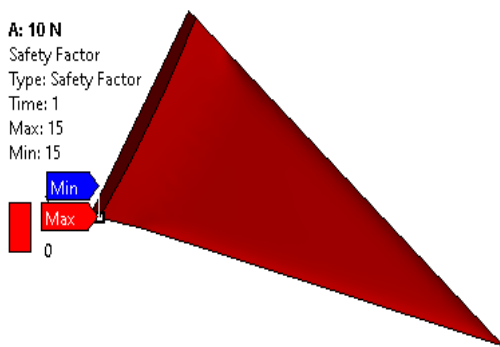


Figure 12. Safety Factor 10 N

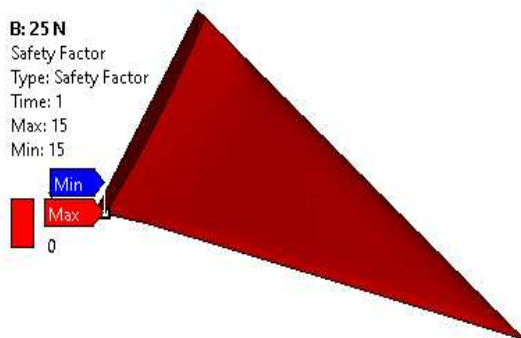


Figure 13. Safety Factor 25 N

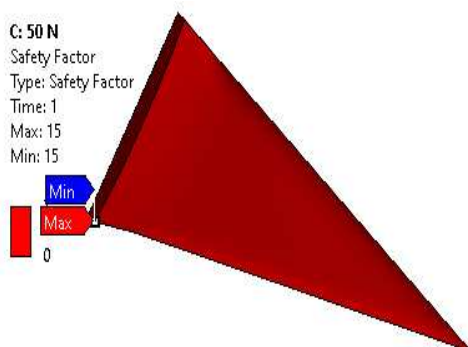


Figure 14. Safety Factor 50 N

CONCLUSION

The distribution of the von Mises stress distribution, deformation at 10N, 25N, and 50N loading variations has risen, according to the results of the analysis and discussion. At 50N loading, the greatest von mises stress and deformation were 0.14755 Mpa and 2.13×10^{-6} m/m. The safety factor result for each variant is 15, indicating that the weed weeding blade structure is exceptionally safe and can handle a load of up to 50 N. As a weed weeding machine blade, the steel construction blade model is recommended.

REFERENCES

- [1] S. K. Mandal, B. Bhattacharyya, S. Mukherjee, and S. Karmakar, "Design Optimisation of Rotary Tiller Blade Towards Service Life Enhancement," *Journal of Manufacturing Engineering*, vol. 16, no. 4, pp. 115–123, 2021, doi: 10.37255/jme.v16i4pp115-123.
- [2] B. Devojee, S. Meena, A. Sharma, and C. Agarwal, "Performance evaluation of weeder by number of blades per flange in chilli crop," *International Journal of Chemical Studies*, vol. 8, no. 2, pp. 727–731, 2020, doi: 10.22271/chemi.2020.v8.i2k.8855.
- [3] R. K.T., "Development of Power Weeder for Line Sown Paddy Crop," *International Journal of Agriculture Environment and Biotechnology (IJAEB)*, vol. 12, no. 3, pp. 261–265, 2019, doi: 10.30954/0974-1712.08.2019.9.
- [4] B. Chirende, J. Q. Li, and W. Vheremu, "Application of finite element analysis in modeling of bionic harrowing discs," *Biomimetics*, vol. 4, no. 3, pp. 1–11, 2019, doi: 10.3390/biomimetics4030061.
- [5] Q. Lai, Q. Yu, and J. Dong, "Dynamic analysis of rotary tiller gearbox based on EDEM, ADAMS and ANSYS," *Journal of Intelligent & Fuzzy Systems*, vol. 36, no. 2, pp. 1153–1160, 2019, doi: 10.3233/JIFS-169889.
- [6] M. A. Matin, M. I. Hossain, M. K. Gathala, J. Timsina, and T. J. Krupnik, "Optimal design and setting of rotary strip-tiller blades to intensify dry season cropping in Asian wet clay soil conditions," *Soil and Tillage Research*, vol. 207, no. October 2020, p. 104854, 2021, doi: 10.1016/j.still.2020.104854.
- [7] S. Lu, H. Jin, M. He, and Z. Xu, "Analysis system of power tiller's general machine components based on VB and ANSYS," *Journal of Physics: Conference Series*, vol. 1237, no. 4, pp. 1–6, 2019, doi: 10.1088/1742-6596/1237/4/042054.
- [8] A. Kešner, R. Chotěborský, M. Linda, M. Hromasová, E. Katinas, and H. Sutanto, "Stress distribution on a soil tillage machine frame segment with a chisel shank simulated using discrete element and finite element methods and validate by experiment," *Biosystems Engineering*, vol. 209, pp. 125–138, 2021, doi: 10.1016/j.biosystemseng.2021.06.012.
- [9] H. Azimi-Nejadian, S. H. Karparvarfard, M. Naderi-Boldaji, and H. Rahmadian-Koushkaki, "Combined finite element and statistical models for predicting force

- components on a cylindrical mouldboard plough," *Biosystems Engineering*, vol. 186, pp. 168–181, 2019, doi: 10.1016/j.biosystemseng.2019.07.007.
- [10] Z. Yin and L. Xu, "Finite element analysis and optimization design of paper cutter cutting blade based on ANSYS," *Proc. - 2018 Int. Conf. Robot. Intell. Syst. ICRIS 2018*, pp. 475–478, 2018, doi: 10.1109/ICRIS.2018.00125.
- [11] T. U. Rehman, M. S. Mahmud, Y. K. Chang, J. Jin, and J. Shin, "Current and future applications of statistical machine learning algorithms for agricultural machine vision systems," *Computers and Electronics in Agriculture*, vol. 156, no. December 2018, pp. 585–605, 2019, doi: 10.1016/j.compag.2018.12.006.
- [12] A. B. Prasetyo, K. A. Sekarjati, and S. Haryo, "Design And Analysis of The Effect of Variation Of compression Force on Allen Key Using Finite Element Analysis Method," *Scientific Journal of Mechanical Engineering Kinematika (SJME Kinematika)*, vol. 7, no. 1, pp. 39–52, 2022, doi: 10.20527/sjmekinematika.v7i1.
- [13] I. G. Torre, J. C. Losada, R. J. Heck, and A. M. Tarquis, "Multifractal analysis of 3D images of tillage soil," *Geoderma*, vol. 311, pp. 167–174, 2018, doi: 10.1016/j.geoderma.2017.02.013.
- [14] X. Jiang, J. Tong, Y. Ma, and J. Sun, "Development and verification of a mathematical model for the specific resistance of a curved subsoiler," *Biosystems Engineering*, vol. 190, pp. 107–119, 2020, doi: 10.1016/j.biosystemseng.2019.12.004.
- [15] M. Askari and Y. Abbaspour-Gilandeh, "Assessment of adaptive neuro-fuzzy inference system and response surface methodology approaches in draft force prediction of subsoiling tines," *Soil and Tillage Research* vol. 194, no. July, p. 104338, 2019, doi: 10.1016/j.still.2019.104338.
- [16] X. Chen and Y. Liu, *Finite element modeling and simulation with ANSYS workbench*. London: CRC Press Taylor & Francis Group, 2019.
- [17] A. B. Prasetyo and K. A. Sekarjati, "Finite Element Simulation of Power Weeder Machine Frame," *Indonesian Journal of Computing, Engineering and Design*, vol. 4, no. 2, pp. 26–34, 2022, doi: 10.35806/ijoced.v4i2.291.
- [18] F. Anggara, D. Romahadi, A. L. Avicenna, and Y. H. Irawan, "Numerical analysis of the vortex flow effect on the thermal-hydraulic performance of spray dryer," *SINERGI*, vol. 26, no. 1, p. 23, 2022, doi: 10.22441/sinergi.2022.1.004.
- [19] S. Y. Tadeuz Stolarski, Y. Nakasone, *Engineering Analysis with ANSYS Software*, 1th ed. London: Elsevier Butterworth-Heinemann, 2006.
- [20] Huei Huang Lie, *Finite Element Simulations with ANSYS Workbench 2021*. Taiwan: Stephen Schroff, 2021.
- [21] N. B. Dantulwar, R. G. Maske, and J. T. Patel, "Finite Element Analysis of Ball Valve Assembly for Earthquakes," *International Conference on Ideas, Impact and Innovations in Mechanical Engineering*, vol. 5, no. 6, pp. 1460–1467, 2017.
- [22] P. Dechaumphai and S. Sucharitpwatskul, *Finite Element Analysis with ANSYS Workbench*. Oxford: Alpha Science International Ltd., 2018.
- [23] M. M. Doustdar and H. Kazemi, "Effects of fixed and dynamic mesh methods on simulation of stepped planing craft," *Journal of Ocean Engineering and Science*, vol. 4, no. 1, pp. 33–48, 2019, doi: 10.1016/j.joes.2018.12.005.
- [24] M. Sosnowski, "The influence of computational domain discretization on CFD results concerning aerodynamics of a vehicle," *Journal of Applied Mathematics and Computational Mechanics*, vol. 17, no. 1, pp. 79–88, 2018, doi: 10.17512/jamcm.2018.1.08.
- [25] M. Sosnowski, J. Krzywanski, and R. Scurek, "A fuzzy logic approach for the reduction of mesh-induced error in CFD analysis: A case study of an impinging jet," *Entropy*, vol. 21, no. 11, 2019, doi: 10.3390/e21111047.
- [26] A. B. Prasetyo and F. Fauzun, "Numerical study of effect of cooling channel configuration and size on the product cooling effectiveness in the plastic injection molding," *MATEC Web Conf.*, vol. 197, pp. 8–11, 2018, doi: 10.1051/mateconf/201819708019.
- [27] M. García Pérez and E. Vakkilainen, "A comparison of turbulence models and two and three dimensional meshes for unsteady CFD ash deposition tools," *Fuel*, vol. 237, no. September 2018, pp. 806–811, 2019, doi: 10.1016/j.fuel.2018.10.066.
- [28] H. Chen, X. Zhou, Z. Feng, and S. J. Cao, "Application of polyhedral meshing strategy in indoor environment simulation: Model accuracy and computing time," *Indoor and Built Environment*, vol. 0, no. 0, pp. 1–13,

- 2021, doi: 10.1177/1420326X211027620.
- [29] M. Sosnowski, J. Krzywanski, K. Grabowska, and R. Gnatowska, "Polyhedral meshing in numerical analysis of conjugate heat transfer," *EPJ Web of Conferences*, vol. 180, pp. 4–9, 2018, doi: 10.1051/epjconf/201817002096.
 - [30] Vutton D. V., *Fundamentals of Finite Element Analysis*, 1st ed. McGraw-Hill Science/Engineering/Math, 2003.
 - [31] B. C. Yemineni, J. Mahendra, J. Nasina, L. Mahendra, L. Shivasubramanian, and S. B. Perika, "Evaluation of Maximum Principal Stress, Von Mises Stress, and Deformation on Surrounding Mandibular Bone During Insertion of an Implant: A Three-Dimensional Finite Element Study," *Cureus*, vol. 12, no. 7, pp. 1–17, 2020, doi: 10.7759/cureus.9430.
 - [32] R. G. Karmankar, "Analysis of Von- Mises-Stress for Interference Fit and Pull- Out States By Using Finite Element Method," *International Research Journal of Engineering and Technology (IRJET)*, vol. 4, no. 11, pp. 1367–1374, 2017, doi: 10.13140/RG.2.2.26447.79520.
 - [33] S. H. Pranoto and M. Mahardika, "Design and finite element analysis of micro punch CNC machine modeling for medical devices," *AIP Conference Proceedings*, vol. 1941, no. March, 2018, doi: 10.1063/1.5028079.
 - [34] N.-H. Kim, B. V. Sankar, and A. V. Kumar, *Introduction to Finite Element Analysis and Design - 2nd Edition*, 2nd Ed. United States of America: Jhon Wiley & Sons, Inc., 2018.
 - [35] J. Pratama and M. Mahardika, "Finite element analysis to determine the stress distribution, displacement and safety factor on a microplate for the fractured jaw case," *AIP Conference Proceedings*, vol. 1941, pp. 1–7, 2018, doi: 10.1063/1.5028080.
 - [36] Ioannis Koutromanos, *Fundamentals of Finite Element Analysis*, 1th ed. London: John Wiley & Sons Ltd All, 2018.
 - [37] X. Wang, Q. Shi, W. Fan, R. Wang, and L. Wang, "Comparison of the reliability-based and safety factor methods for structural design," *Applied Mathematical Modelling*, vol. 72, pp. 68–84, 2019, doi: 10.1016/j.apm.2019.03.018.
 - [38] I. Elishakoff, *Safety Factors and Reliability: Friends or Foes*, 1st ed. Florida: Springer Science Business Media, 2004.
 - [39] K. Z. V. Dobrovolsky, *Machine Elements : a textbook*. Moscow: Peace, 1973.
 - [40] L. A. N. Wibawa, K. Diharjo, W. W. Raharjo, and B. H. Jihad, "Stress analysis of thick-walled cylinder for rocket motor case under internal pressure," *Journal of Advanced Research in Fluid Mechanics and Thermal Sciences*, vol. 70, no. 2, pp. 106–115, 2020, doi: 10.37934/ARFMTS.70.2.106115.
 - [41] L. A. N. Wibawa, K. Diharjo, W. W. Raharjo, and B. H. Jihad, "The effect of fillet radius and length of the thick-walled cylinder on von Mises stress and safety factor for rocket motor case," in *AIP Conference Proceedings*, 2020, vol. 2296, no. November, pp. 1–8, doi: 10.1063/5.0030329.